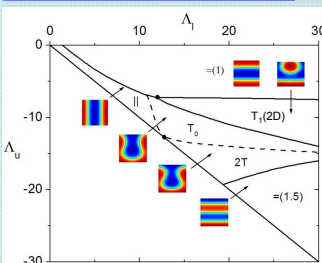


Part I. Symmetric DBC ($f_A=0.5$) Thin Films



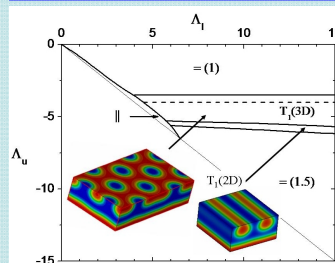
A_s : surface preference - $A_s > 0$ prefers A, $A_s < 0$ prefers B, $A_s = 0$ is neutral.

2D Phase Diagram at $D=L_0$ (with Hard-Surface Effect)



◆ The transitions among ||, T_1 and 2T are of the second order.
◆ Mixed morphologies ($T_1(2D)$, T_2 and 2T) form due to their subtle balance among chain entropy, A-B repulsion, and surface energies.

3D Phase Diagram at $D=L_0$ (without Hard-Surface Effect, $\phi(r)=1$)



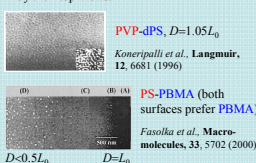
◆ A novel 3D mixed morphology $T_3(3D)$ is found, which has smaller A-B repulsion than $T_1(2D)$.

Three effects of confining surfaces:

1. The surface preference for one of the blocks favors parallel lamellae.
2. The surface confinement favors perpendicular lamellae when the surface separation D is incommensurate with the bulk lamellar period L_0 .
3. The hard-surface effect favors perpendicular lamellae. This is due to the presence of impenetrable (hard) walls, at which the overall polymeric segmental density ϕ_1 is reduced to 0 (from 1 in the interior of the film). Chains also lose conformational entropy near hard walls. (D. Meng and Q. Wang, *J. Chem. Phys.*, 126, 234902 (2007))

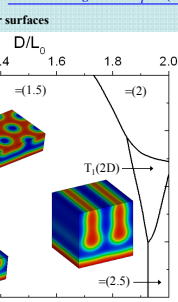
Possible Experimental Evidence of $T_3(3D)$

◆ $T_3(3D)$ can be distinguished from $T_1(2D)$ and || by their top-views.



PVP-dPS, $D=1.05L_0$ (Konerjallil et al., *Langmuir*, 12, 6681 (1996))
PS-PBMA (both surfaces prefer PBMA) (Fassella et al., *Macromolecules*, 33, 5702 (2000))
 $D=0.5L_0$ $D=L_0$

3D Phase Diagrams at $\Lambda=15$ (without Hard-Surface Effect, $\phi(r)=1$)



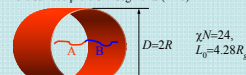
◆ In the above, $T_2(3D)$ is similar to $T_1(3D)$ but has two parallel A-B interfaces near the lower surface and an inverted A-B pattern near the upper surface. $T_1(2D)$ between similar surfaces has different A-B interfacial curvatures near the upper surface than those in $T_1(2D)$ between dissimilar surfaces.

◆ In the left, the stable region of mixed morphology ($T_1(3D)$ and $T_1(2D)$) shrinks as D increases from L_0 , and vanishes for $D > 1.2L_0$. As D further increases towards $2L_0$, $T_2(2D)$ appears as the only stable mixed morphology and has prolonged perpendicular A-B interfaces compared to $T_1(2D)$ at $D=L_0$, which help alleviate the frustration at the T-junctions.

D. Meng and Q. Wang, *Soft Matter*, submitted

Part III. Symmetric DBC ($f_A=0.5$) in Nano-Pores

Pore surface prefers A segments ($\Lambda > 0$)

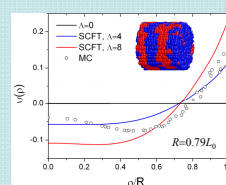


ρ : radial distance from the pore center;
 $\psi(\rho) = \phi_A(\rho) - \phi_B(\rho)$: order parameter.

Lattice Monte Carlo (MC) simulation data are taken from Q. Wang, *J. Chem. Phys.*, 126, 024903 (2007).

At Small Λ : Undulation of A-B Interfaces in Slab Morphology

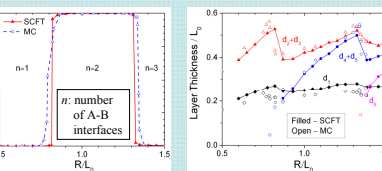
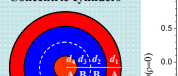
At Intermediate Λ : Morphology Stability via Free-Energy Comparison



◆ Due to the surface preference, A-B interfaces in the slab morphology are undulated so that more A segments can be in contact with the pore surface.

At Large Λ : Structure of Concentric Cylinders

Concentric cylinders



◆ Good agreement between SCF and MC results are found for concentric cylinders.

◆ The mixed morphology was also reported in lattice MC simulations. Our SCF calculations show that this morphology is *unstable* due to its large entropic penalty (chain-stretching).

◆ The parallel morphology was also reported in lattice MC simulations. Our SCF calculations show that this morphology is *unstable* due to its large A-B repulsion.

D. Meng, X. Zhang, and Q. Wang, *Macromolecules*, to be submitted

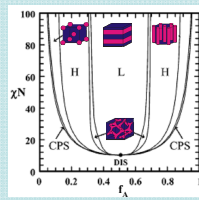
Self-Assembly of Diblock Copolymers (DBC)



A and B segments are assumed to have the same statistical segment length a and bulk density ρ_0 .

- L_0 : Bulk structure period;
- f_A : Volume fraction of A block;
- χ : Flory-Huggins parameter between A and B segments;
- N : Copolymer chain length.

$$R_g = \sqrt{N} a \nu$$



Bulk phase diagram from Cochran et al., *Macromolecules*, 39, 2449 (2006).

Self-Consistent Field (SCF) Calculations

Hamiltonian: $\mathcal{H} = \mathcal{H}_c + \mathcal{H}_r + \mathcal{H}_s$ Canonical ensemble

- \mathcal{H}_c : entropic contribution of copolymer chains;
- \mathcal{H}_r : A-B repulsion described by the χ parameter;
- \mathcal{H}_s : surface-copolymer interactions.

Incompressibility constraint: $\phi_A(r) + \phi_B(r) = \phi(r)$

$\phi(r)$: normalized (by ρ_0) density field of i (A, B) segments;
 $\phi_i(r)$: total segmental density at spatial position r .

Performed in real space without a priori knowledge about possible morphologies.

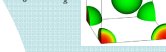
Summary

- ◆ We have performed real-space self-consistent field (SCF) calculations with high accuracy to study the self-assembled morphology of diblock copolymers (DBC) under nano-confinement for several systems, including 1D lamellae-forming DBC confined between two homogeneous and parallel surfaces (thin films), in nano-pores, and on topographically patterned substrates; 2D cylinder-forming DBC on chemically stripe-patterned substrates; and 3D sphere- and gyroid-forming DBC thin films. The stable phases are identified through free-energy comparisons, and our SCF results are compared with available experiments and Monte Carlo simulations.
- ◆ The surface preference, geometry, confinement, and pattern all have significant influence on the self-assembled morphology of DBC under nano-confinement. Much richer phase behaviors are found in all of these systems, with complex morphologies that are very different from those in the bulk.
- ◆ Understanding and predicting the self-assembled morphology of DBC under nano-confinement will help us obtain the desirable morphology for targeted applications. Real-space SCF calculation is a powerful tool for this purpose.

S. M. Park, D. Meng, C. T. Retner, D. S. Dandy, Q. Wang, and H. C. Kim, *Macromolecules*, in press

Part IV. Preliminary Results of Asymmetric DBC Thin-Films Between Identical Surfaces

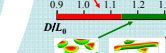
$\chi N = 23.5$
 $f_A = 0.2$
 $L_0 = 4.49R_g$



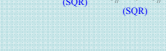
$\chi N = 20$
 $f_A = 0.357$
 $L_0 = 9.50R_g$



$\chi N = 20$
 $f_A = 0.357$
 $L_0 = 9.50R_g$



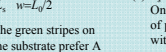
$\chi N = 20$
 $f_A = 0.357$
 $L_0 = 9.50R_g$



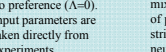
$\chi N = 20$
 $f_A = 0.357$
 $L_0 = 9.50R_g$



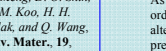
$\chi N = 20$
 $f_A = 0.357$
 $L_0 = 9.50R_g$



$\chi N = 20$
 $f_A = 0.357$
 $L_0 = 9.50R_g$



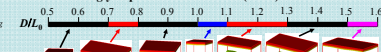
$\chi N = 20$
 $f_A = 0.357$
 $L_0 = 9.50R_g$



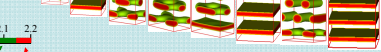
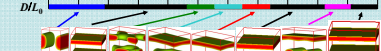
$\chi N = 20$
 $f_A = 0.357$
 $L_0 = 9.50R_g$

Gyroid-Forming DBC

Between strongly A-preferential surfaces ($\Lambda=10$)



Between strongly B-preferential surfaces ($\Lambda=-10$)

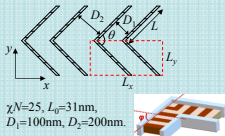


◆ Preliminary SCF calculations are performed without the hard-surface effect, i.e., $\phi(r)=1$.

◆ Various morphologies (cylinders, lamellae, and perforated lamellae) different from the bulk morphology, deformed spheres, and *no* gyroid structure are found in thin films.

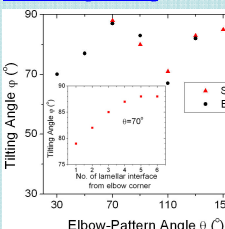
◆ More calculations are needed and on-going.

Part II. Symmetric DBC ($f_A=0.5$) on Topographically Patterned Substrates



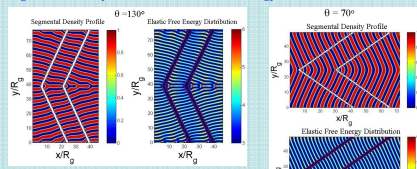
◆ The area enclosed by the red dashed lines is the unit cell used in SCF calculations. We performed 2D calculations in accordance to the experimental setup. All input parameters are taken directly from experiments, where both the sidewalls and substrate are neutral, leading to perpendicular lamellae.

Lamellae Tilting vs. Bending



1. Lamellae tilt at $\phi > 90^\circ$ to alleviate the bending of lamellae. As θ increases from 70° to 110° , reducing the lamellae bending at the cost of increasing lamellae tilting explains the decrease of ϕ .
2. At $\theta=70^\circ$, as the elbow corner is approached, the available space for copolymers become smaller and are structures with smaller ϕ form instead of bend structures with high entropic penalty at the bending vertices. The same reasoning applies when θ is decreased from 70° , explaining the decrease of ϕ in this region.
3. At $\theta=130^\circ$ and larger, the lamellae break and form O-kinks with highly localized entropic penalty. This helps relieve the entropic penalty in other regions. ϕ therefore suddenly increases to about 90° and levels off in this region.

Segmental Density and Chain Elastic Free Energy Distributions from SCFT



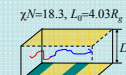
Top-View SEM Images from Experiments



◆ The elastic free energy ($k_B T / \text{chain}$) due to chain conformational entropy is high at bending vertices and Ω -kinks.

S. M. Park, D. Meng, C. T. Retner, D. S. Dandy, Q. Wang, and H. C. Kim, *Macromolecules*, in press

Part V. Cylinder-Forming DBC ($f_A=0.3$) on Chemically Nano-Patterned Substrates



$\chi N = 18.3$, $L_0 = 4.03R_g$

Self-Consistent Field Calculations

◆ Our SCF calculations are in good agreement with experimental observations, and further provide the 3D structures in the films and their formation mechanisms.

(a) $L_s = L_0 = 45\text{nm}$, $D = 40\text{nm}$

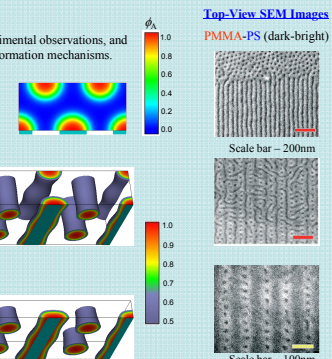
On a commensurate substrate pattern, two layers of parallel half-cylinders form and are registered with the stripe pattern on the substrate.

(b) $L_s = 2.3L_0 = 100\text{nm}$, $D = 40\text{nm}$

On an incommensurate substrate pattern, mixed morphology forms with two layers of parallel half-cylinders on preferential stripes and perpendicular cylinders on neutral stripes.

(c) $L_s = 2.3L_0 = 100\text{nm}$, $D = 20\text{nm}$

As D is reduced by half from (b), well ordered mixed morphology forms with alternating parallel half-cylinders on preferential stripes and perpendicular cylinders on neutral stripes.



Top-View SEM Images

PMMA-PS (dark-bright)

Scale bar - 200nm

Scale bar - 100nm

S. O. Kim, B. H. Kim, D. Meng, D. O. Shin, C. M. Koo, H. H. Solak, and Q. Wang, *Adv. Mater.*, 19, 3271 (2007)